Knockdown of zebrafish Na$_v$1.6 sodium channel impairs embryonic locomotor activities

Yau-Hung Chen[1], Fong-Lee Huang[2], Yi-Chuan Cheng[3], Chia-Jung Wu[4], Cheng-Ning Yang[4] & Huey-Jen Tsay[4,*]

[1]Graduate Institute of Life Sciences, Tamkang University, Taipei, Taiwan; [2]Department of Anatomy, School of Medicine, National Yang-Ming University, Taipei, Taiwan; [3]Department of Biochemistry and Molecular Biology, Chang-Gung University, Taoyuan, Taiwan; [4]Institute of Neuroscience, School of Life Sciences, Brain Research Center, National Yang-Ming University, ROC, No. 155, Sec. 2, Li-Nung Street, Taipei, 112, Taiwan, ROC

Abstract

Although multiple subtypes of sodium channels are expressed in most neurons, the specific contributions of the individual sodium channels remain to be studied. The role of zebrafish Na$_v$1.6 sodium channels in the embryonic locomotor movements has been investigated by the antisense morpholino (MO) knockdown. MO1 and MO2 are targeted at the regions surrounding the translation start site of zebrafish Na$_v$1.6 mRNA. MO3 is targeted at the RNA splicing donor site of exon 2. The correctly spliced Na$_v$1.6 mRNA of MO3 morphants is 6% relative to that of the wild-type embryos. Na$_v$1.6-targeted MO1, MO2 and MO3 attenuate the spontaneous contraction, tactile sensitivity, and swimming in comparison with a scrambled morpholino and mutated MO3 morpholino. No significant defect is observed in the development of slow muscles, the axonal projection of primary motoneurons, and neuromuscular junctions. The movement impairments caused by MO1, MO2, and MO3 suggest that the function of Na$_v$1.6 sodium channels is essential on the normal early embryonic locomotor activities.

Introduction

The voltage-gated Na$_v$1.6 sodium channels expressed abundantly in the central and peripheral nervous system contribute the predominant sodium current determining the firing patterns of rodent Purkinje cells, cortical pyramidal neurons, and motoneurons [1–3]. Mutant mice with different alleles of the Na$_v$1.6 sodium channel which mimic human motor end plate disease (*med*) display a broad spectrum of neurological phenotypes depending on the remaining level of Na$_v$1.6 sodium channels [4, 5]. The decreased high-frequency firing and reduced levels of resurgent and persistent currents are found in Purkinje cells of *med* and Purkinje cell-specific Na$_v$1.6 knockout mice [6, 7]. Na$_v$1.6 sodium channels are also responsible for the postnatal increase of the sodium current in motoneurons [8]. The conduction velocity of the motoneurons is reduced in *med^j* allele of Na$_v$1.6 which contains a mutant splicing donor site [5]. However, the physiological role of Na$_v$1.6 sodium channels in the early developmental stages has not yet been studied.

Zebrafish Na$_v$1.6 sodium channels are expressed in trigeminal ganglia, hindbrain, Rohon-Beard (RB) neurons, interneurons, and motoneurons which form the functional circuit mediating the tactile response [9, 10]. The peak sodium current amplitude in RB neurons is attenuated and tactile sensitivity was reduced at 48 hpf by Na$_v$1.6

*To whom correspondence should be addressed. Fax: +886-2-28200259; E-mail: hjtsay@ym.edu.tw

morpholino knockdown which suggested that the developmental upregulation of zebrafish $Na_v1.6$ sodium channels is physiologically significant [11]. Furthermore, the $Na_v1.6$ knockdown leads to the delayed axonal projection of the secondary motoneurons [12]. Due to the transparency of zebrafish embryos, the locomotion during the development has been thoroughly documented including the alternating coiling contractions (side-to-side contractions) which initiates at 17 h post-fertilization (hpf), the touch-evoked rapid coiling (escape) which initiates at 21 hpf, and the organized swimming which initiates at 26 hpf [13]. The well characterized motor circuit makes zebrafish a valuable model system for investigating the specific function of $Na_v1.6$ sodium channels during the early embryonic development [14]. In the present study, we show that the knockdown of $Na_v1.6$ leads to the impaired alternating coiling contractions, touch-evoked coiling, and swimming without impeding the axonal projection of primary motoneurons, the development of slow muscles, and the neuromuscular junctions.

Materials and methods

Animals

Adult zebrafish (*Danio rerio*, Oregon AB line) from the Institute of Zoology, Academia Sinica, Taiwan were used as the breeding stock. Embryos were staged by hours or days of post fertilization (hpf, dpf). Embryos were raised in the embryonic medium (EM) containing phenylthiourea. To block all of sodium channels, 0.006% tricaine was added into EM at 16 hpf and remained in EM-PTU at 28 °C until the experimental stages.

Sequence-targeted morpholinos and microinjection

Morpholinos (MO) were synthesized by Gene Tools (Corvallis, OR) based on the zebrafish $Na_v1.6$ genomic sequence [9]. MO1 and MO2 were designed to block the translation of $Na_v1.6$, while MO3 was designed to block the splicing of $Na_v1.6$ premature mRNA. MO3mis morpholino was synthesized by introducing mismatches at five positions of MO3. MO1 (5′-TgCAgCAACTTCTTCTCCTgTTATg-3′) and MO2 (5′-TACCCTCCACggCAg CCAgTT TATg-3′) were located at 11–35 bp and 36–60 bp

upstream of ATG, respectively. MO3 (5′-gTgAT ACTgCACTCACTT TCTgATT-3′) was located at the exon 2-intron 2 boundaries. MO3mis (5′-gTCA TACTCCAgTCag TTTCTCATT-3′) and SMO, an unrelated scrambled sequence, (5′-CCTCTTACCT CAgTTACAATTTATA-3′) were utilized as injection controls. Fertilized eggs were injected into the interphase of cell and yolk using an oil-driven microinjector (Drummond).

Quantitative PCR and RT-PCR analysis

Total RNA was purified from MO3, MO3mis-injected, and wild type embryos at 27 hpf using the TRIZOL® reagent (Invitrogen). One-step quantitative PCR was performed using Titanium One-Step RT-PCR kit (Clontech). The level of normally spliced transcripts was analyzed using a forward primer (PI, 5′-gAgAAgCgTATCgAggAggAg-3′) located at exon 2 and reverse primer (PII, 5′-gAT TgTTTTCCCTTTATTTAggAC-3′) located at exon 3, and the PCR product is a 233-bp DNA fragment. The level of Elongation factor 1a (EF1a) mRNA was analyzed to normalize the amount of RNA used for PCR. The forward and reverse primers for EF1a were 5′-gCTCAAggAgAAgATCgACCgT-3′ and 5′-CAgCAAAg CgACCAAgAggAgg-3′, respectively. The conditions were 30 min at 50 °C; 10 min at 94 °C for the initial melting; 40 cycles at 95 °C for 10 s, 60 °C for 10 s, 68 °C for 10 s, followed by 10 min at 68 °C and 1 min at 99 °C. The RT-PCR products were analyzed by gel electrophoresis.

Motility recording

The in-chorion movement of zebrafish embryos was analyzed using a digital camera (Nikon DXM 1200) mounted on a microscope (Nikon 800). The definition of in-chorion contractions was based on the angle of the tail displacement relative to the body axis. Embryos with the tail movements from one side to the other side at an angle $> 90°$, an angle $> 45°$, and an angle of $< 45°$ on one side were classified as having side-to-side, single-side, and slight movements, respectively. To quantify the in-chorion behavior, both single-side movements and slight movements were scored as 1; while a side-to-side contraction was scored as 2.

Larvae at 33 hpf were placed in the 6 cm Petri dishes and videotaped using a video camera mounted on a dissecting microscope. The coil-coiled

contractions were initiated by tactile stimulation to the region near the trigeminal neurons. Ten tactile stimuli with 5 s intervals were applied. A full contraction was defined as a contraction in which the tail touched the head. Larvae at 36 hpf were placed within a circle with a 2 mm diameter in the 60 mm Petri dish. The swimming behaviors were initiated by tactile stimulation, and the number of times a larva swam out of the circle was counted for 20 stimuli with 5 s intervals.

Whole-mount in situ hybridization and immunohistochemistry

Embryos were fixed in 4% paraformaldehyde and immunohistochemistry was performed as previously described [15]. Briefly, embryos were incubated overnight with znp1 (Developmental Hybridoma Bank, University of Iowa, IA) and the anti-slow muscle-specific myosin heavy chain antibody, F59 [16, 17] at the dilutions of 1:500 and 1:10, respectively. After washed with PBS, embryos were incubated in the FITC-conjugated secondary antibody (Jackson Laboratory) (1:500 diluted in 0.1% Tween-20 in phosphate-buffered saline; PBST) overnight at 4 °C, and washed in PBST. The secondary motoneurons were visualized by using antibody zn5 (Developmental Hybridoma Bank, University of Iowa, IA). The bound antibody was visualized by biotinylnated secondary antibody using the ABC kit. DAB coloring was performed with and without nickel enhancement. To investigate the migration of slow muscles, the embryos were embedded in agar-sucrose (1.5% agar and 5% sucrose) and sectioned. Whole embryos and sections were visualized under Zeiss Axioplan 2 microscope. In situ hybridization using $Na_v1.6$ specific probe was performed as described previously [9].

Acetylcholine receptor clustering

α-Bungarotoxin (α-BTX) labeling of acetylcholine receptor (AChR) was performed as previously described [18]. Briefly, embryos were fixed in 4% paraformaldehyde in phosphate-buffered saline (PBS) for 4 h at room temperature, and then washed in PBST. Fixed embryos were digested in 0.1% collagenase (Sigma-Aldrich) and washed in PBST. Embryos were incubated for 30 min at room temperature in 10 µg/ml Rhodamine-conjugated α-BTX (Molecular Probe, Eugene, OR)

diluted in NCS-PBST (10% normal calf serum and 1% DMSO in PBST), and then washed in PBST. α-BTX-labeled embryos were incubated with znp1 antibody to locate motoneurons. Embryos were mounted in Vectashield (Vector, CA) and images taken using a Leica confocal microscope (DMRE) were compiled.

Statistical analysis

The data was analyzed by the analysis of variance (ANOVA) using the statistical analysis system (SAS, SAS Institute, Cary, NC) followed by Fisher's post-hoc least significant difference (LDS) test, and presented as mean $\pm$ SEM. A p value of < 0.05 was considered statistically significant.

Results

Knockdown of zebrafish $Na_v1.6$ sodium channels by antisense morpholinos severely impaired embryonic motilities

The role of zebrafish $Na_v1.6$ sodium channels was studied using the antisense morpholinos targeted to the different positions of the $Na_v1.6$ mRNA (Figure 1A). The sequence-specific MO1 and MO2 were designed to prevent the ribosome binding to $Na_v1.6$ mRNA. The exon-intron (splicing donor)-targeted MO3 was designed to block the splicing of $Na_v1.6$ intron. The blocking intron 2 splicing by MO3 and MO3mis morpholino at 27 hpf were shown by RT-PCR (Figure 1C). PI and PII primer were located at the second and third exon (Figure 1B) and the length of the spanning intron was 4 kb. A 233-bp DNA fragment was detected in wild type embryos and MO3mis morphants. The spliced mRNA was almost undetectable in MO3 morphants (Figure 1C, lane 3). The result of quantitative PCR indicated that the relative level of spliced mRNA in wild-type embryos, MO3, and MO3mis morphants were 100.0 ± 14.5, 6.1 ± 0.4, and 25.5 ± 1.6%, respectively. MO3 effectively attenuated the splicing process of the endogenous $Na_v1.6$ mRNA. Surprisingly, the level of spliced mRNA of MO3mis morphants did not restore the level of $Na_v1.6$ mRNA, which suggests that MO3mis with the 5-base mismatch still contained certain binding ability to the splicing site. To investigate whether
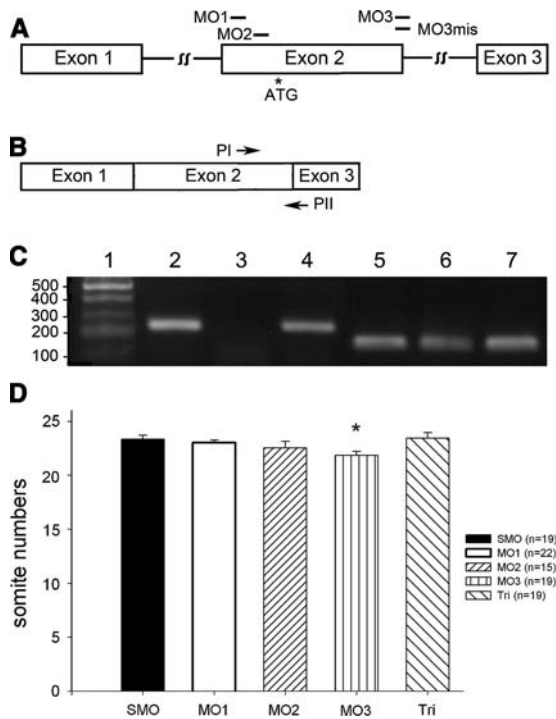
Figure 1. Target sites of Na$_v$1.6 MOs and the reduced transcript of Na$_v$1.6 mRNA in MO3 morphants. (A) The locations of sequence-specific morpholinos of MO1, MO2, MO3, and MO3mis. (B) The locations of PI and PII primers utilized in RT-PCR and Quantitative PCR analysis. (C) Lane 1 represents the molecular weight markers. Lanes 2–4 represents the RT-PCR products of RNA prepared from wild type, MO3, and MO3mis morphants using the PI and PII primers. The reduced level of the corrected spliced Na$_v$1.6 mRNA was detected in MO3 morphants than that of the wild type and MO3mis embryos. The level of EF1a mRNA was used as a normalizing control for RT-PCR. Lanes 5–7 represents the PCR products of the RNA prepared from wild type, MO3, and MO3mis morphants using the EF1a-specific primers. (D) The somite number was counted using embryos stained with the slow muscle-specific antibody F59. The somite numbers of MO1 and MO2 morphants and tricaine-treated embryos except for the MO3 morphants were similar to SMO controls at 22 hpf (*$P < 0.05$).

the morpholino injection leaded to the general developmental delay, the somite numbers of 22 hpf embryos were counted (Figure 1D). Morpholinos with a scrambled sequence (SMO) and embryos treated with tricaine, a broad VGSC blocker, were used as the control groups. The somite numbers of SMO, MO1, MO2, MO3, and tricaine-treated embryos were 23.3 ± 0.1, 23.0 ± 0.3, 22.5 ± 0.6, 21.8 ± 0.4, and 23.4 ± 0.5, respectively. No significant differences were found among SMO, MO1, MO2, and tricaine-treated embryos. However, the somite number of MO3 morphants was slightly

reduced. This data suggested that the injections of MO1 and MO2 morpholino or tricaine treatment did not lead to the significant developmental delay.

Spontaneous coiling contractions (side-to-side contractions) are mediated by the electrically coupled network [19]. MO morphants displayed different extents of defects in the in-chorion contractions at different morpholino injection doses. At the 3 ng injection dose, 77.8% ($n = 635$), 75.8% ($n = 959$), and 74.7% ($n = 994$) of MO1, MO2, and MO3 morphants failed to exhibit alternating side-to-side contractions. In contrast, all of SMO ($n > 400$) morphants were capable of generating alternating side-to-side contractions. To further analyze the behavioral defects, in-chorion contractions of SMO and MO morphants were recorded at 24 hpf. The percentage of side-to-side movement, single-side movement, and slight movement during the 3-min observation were compared among SMO, MO1, MO2, MO3, and MO3mis (Figure 2A). The behavior scores in MO1, MO2, and MO3 morphants were 2.0 ± 0.9, 2.1 ± 0.6, and 6.1 ± 1.1, respectively. The behavior scores of SMO and MO3mis embryos were 20.9 ± 1.5 and 19.1 ± 1.3 (Figure 2B). This data suggested that Nav1.6 sodium channels played an important role in the electrically coupled network.

Zebrafish exhibits up to three alternating coils in response to a single touch stimulus which required the chemically coupled locomotor network [13]. SMO-injected embryos displayed vigorous contractions at 33 hpf and MO1 morphants responded a touch slightly. The number of alternating coils induced by touches was calculated (Figure 2C). Compared with SMO morphants, MO morphants exhibited significantly reduced touch sensitivity. The role of Na$_v$1.6 in touch-evoked swimming behavior was examined at 36 hpf. The average number of times the SMO morphants swam out of the field was 8.2 ± 0.5 with 20 stimuli. The average number of times for MO1, MO2, and MO3 morphants were 2.8 ± 3.1, 0.2 ± 0.7, and 0.5 ± 2.2, respectively (Figure 2D). These data suggested that Na$_v$1.6 knockdown also attenuated tactile sensitivity.

CaP axonal projections and alignment of muscle fibers were not defective in Na$_v$1.6 morphants

Both altered structures of motor circuits and defective transmission of action potentials could lead to locomotion defects in MO morphants. The axonal projection of motoneurons was examined.
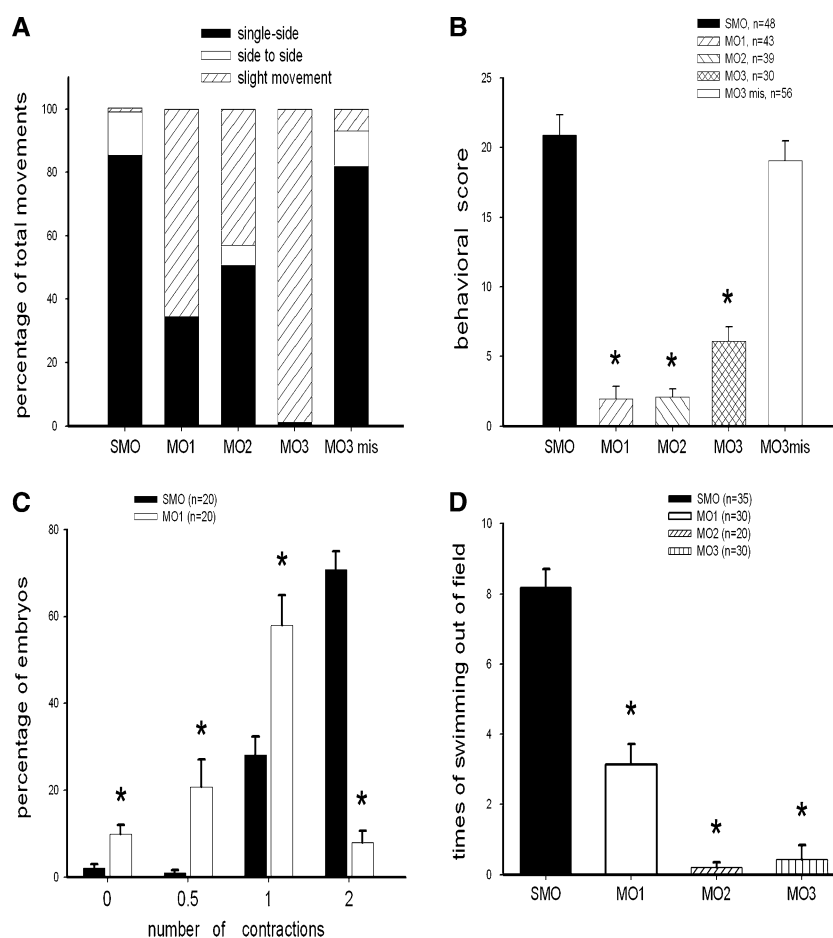
Figure 2. The in-chorion contractions and tactile responses were defective in the MO morphants in comparison with SMO and MO3mis morphants. (A) The percentages of the three classified in-chorion contractions (slight movement, black; single-side movement, white; and side-to-side movement, hatch) were analyzed at 24 hpf. The major activity elicited by the MO1, MO2, and MO3 morphants was the slight movement during the 3-min recording. (B) The behavioral scores of SMO, MO1, MO2, MO3, and MO3-mis morphants were recorded at 24 hpf. The behavioral scores were significantly reduced in the MO1, MO2, and MO3 morphants (*$P < 0.05$). (C) The percentages of the movements with no-response, half-coil, one-coil, and more than two coils elicited by the tactile stimuli. (D) The times of MO1, MO2, and MO3 morphants swam out of the 2-mm circle in response to 20 touches (*$P < 0.05$).

CaP axonal trajectories of MO3 ($n = 25$) and MO3mis ($n = 25$) morphants were similar to those of SMO ($n = 30$) and tricaine-treated ($n = 57$) embryos at 24 hpf (Figure 3A). To determine whether the locomotion defects of MO morphants were due to the muscle malformation, the slow muscle morphology was examined using antibody F59. No alignment difference of slow muscle fibers between SMO, MO1, MO3, and MO3mis morphants was observed at 27 hpf (Figure 3B). In contrast to the normal muscle fibers of SMO, MO3, and MO3mis morphants, the wavy slow-muscle morphology was observed in tricaine-treated embryos. The cross-sections of embryos

showed that F59-positive, slow-muscle fibers migrated to the lateral surface of the trunk in SMO, MOs-injected, and tricaine-treated embryos (insets of Figure 3B). The migration of slow muscle toward the final destination was not affected in all embryos; despite the wavy slow-muscle fibers induced by tricaine treatment.

No major defect in AChR clustering was observed in Na$_v$1.6 morphants

Several studies in mammals have shown that electrical activity modulates neuromuscular synaptic connections [20]. We have examined whether the
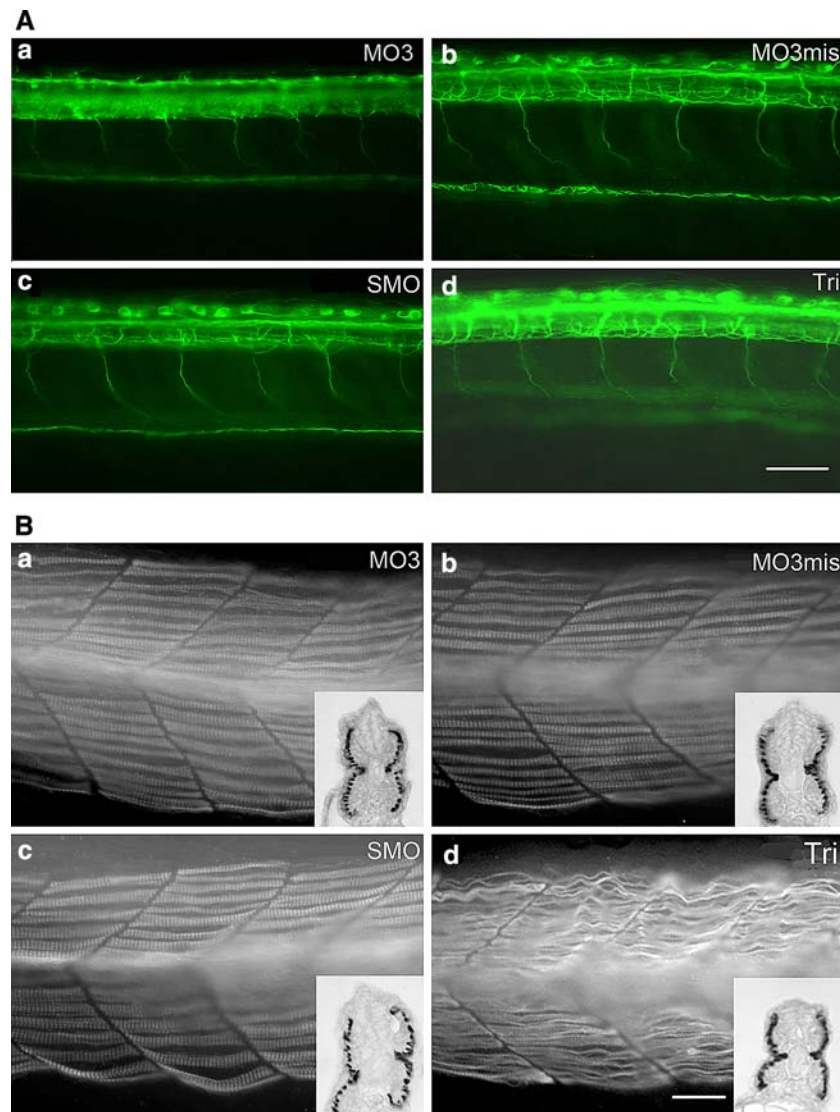
Figure 3. No significant defect was observed in the axonal projections of CaP and the slow muscle development in MOs morphants. (A) The lateral views of embryos stained with znp1 at 27 hpf (anterior left). All of the CaP axons in SMO, MO3, MO3mis morphants and tricaine-treated embryos projected to the ventral trunk (somite 10 to 15) at 27 hpf ($n > 25$). Scale bar was 40 μm. (B) The lateral views of embryos stained with F59 for the alignment of the slow-muscle fibers in the SMO, MO1, MO3, and MO3-mis morphants, and tricaine-treated embryos at 27 hpf. Insets were the cross-sections of F59-stained embryos. The anterior was to the left and dorsal was up. Scale bar was 20 μm.

formation of neuromuscular junctions was affected by the knockdown of $Na_v1.6$. The AChR (acetylcholine receptor) clusters and motoneuron projections were stained with α-bungarotoxin (Figure 4A, D G, J) and antibody znp1 (Figure 4B, E, H, K) at 72 hpf. Neuromuscular junctions shown by the overlapping signals of α-bungarotoxin and motoneuron were observed in MO3, and MO3mis, SMO morphants, and tricaine-treated larvae (Figure 4C, F, J, L). These results suggested that reduced electrical activity did not block the formation of neuromuscular connections.

The delayed expression of $Na_v1.6$ mRNA in the secondary motoneurons precluded the involvement of secondary motoneurons in impaired locomotions of $Na_v1.6$ morphophants

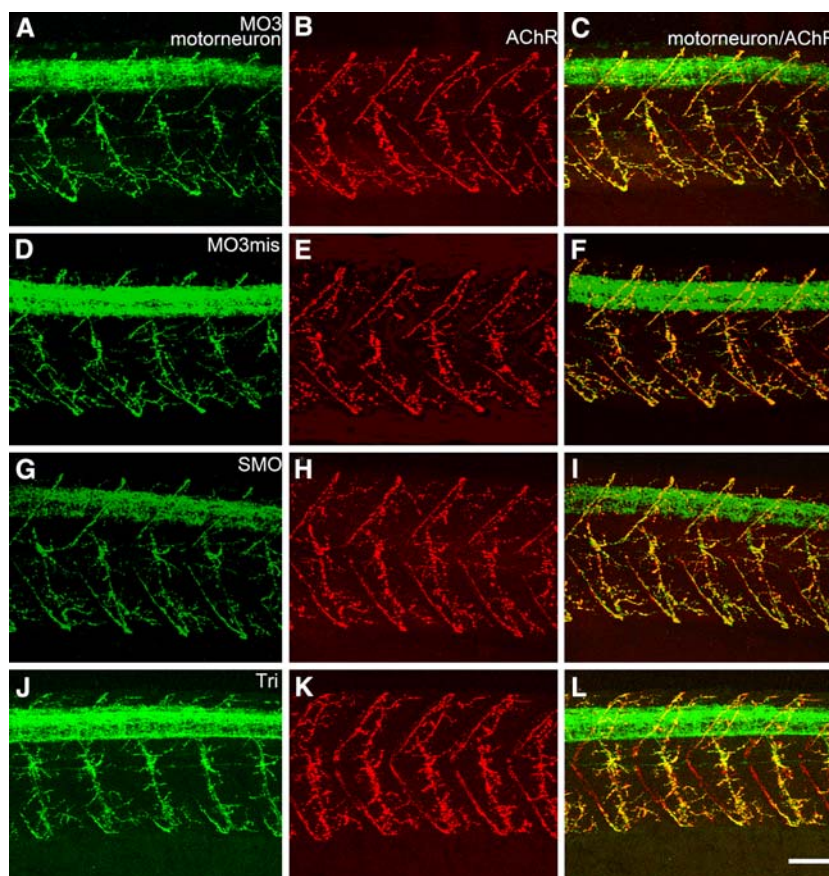Pineda et al. have showed that $Na_v1.6$ was expressed in the dorsal projecting secondary

Figure 4. No significant defect in the AChR clustering was observed in the MOs morphants at 72 hpf under the confocal micro-scope. The axonal morphology of motoneurons was shown by using antibody znp1 (A, D, G, and J). The AChR clusterings were shown by using α-bungarotoxin staining (B, E, H, and K). The compiled confocal images of the znp1 staining and α-bungarotoxin showed that the motor axonal projections were branched and overlapped mostly with the clusters of AChR (C, F, I, and L). The anterior was to the left and dorsal was up. Scale bar was 50 μm.

motoneurons (SMN) [12]. We next examined whether the defective motor activities observed in this study have a temporal correlation with the expression of $Na_v1.6$ in SMN. Neurolin recognized by antibody zn5 is expressed in SMN, but not in primary motoneurons. At 36 hpf, SMN were stained heavily by antibody zn5 at the ventral region of the spinal cord. However, $Na_v1.6$ mRNA was almost undetectable in the zn5-positive region of the spinal cord (Figure 5A, B). The cross-section of whole-mount embryos confirmed that zn5-positive neurons were not overlapped with neurons expressing $Na_v1.6$ mRNA in the spinal cord (Figure 5 C and D). At both 48 and 72 hpf, the levels of $Na_v1.6$ mRNA in zn5-positive SMN remained low (Figure 5 E–J). The expression of $Na_v1.6$ became abundant in the ventral region of the spinal cord at 5 dpf (Figure 5 K–N). Since

in-chorion contraction and tactile/swimming movements were performed prior to 36 hpf, the involvement of SMN in the impaired motilities of MO morphants was excluded.

Discussion

Different neurological disorders are exhibited by the individual null mutations of $Na_v1.1$, $Na_v1.2$, $Na_v1.6$, and $Na_v1.8$ sodium channels which demonstrate that the functions of these sodium channel subtypes are not redundant [21–24]. The subtypes of sodium channels contain unique properties on shaping the specific neuronal activities [22, 25]. The global null mutations of the $Na_v1.1$, $Na_v1.2$, and $Na_v1.6$ are lethal which preclude the analysis of their physiological roles.
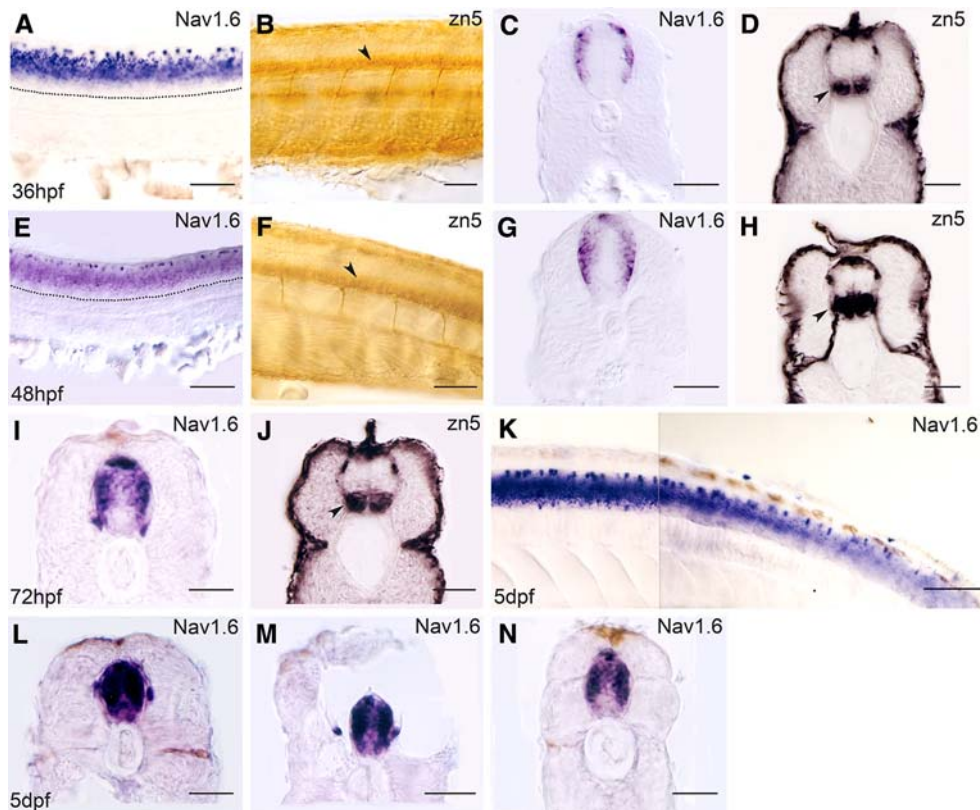
Figure 5. The temporal expression patterns of zebrafish Na$_v$1.6 in the secondary motoneurons. The antisense riboprobes containing the C-terminal and 3′ noncoding regions (5617–6529 nt) were used for the in situ hybridization. The anterior was to the left. A, B showed the lateral view and C, D were the cross-sections of the in situ hybridization and zn5 immunoreactivity in the spinal cord at 36 hpf. The dotted line marked the boundary of notochord and spinal cord. E and F showed the lateral view, and G and H were the cross-sections of the in situ hybridization and zn5 immunoreactivity in the spinal cord at 48 hpf. I and J were the cross-sections of the in situ hybridization and zn5 immunoreactivity in the spinal cord at 72 hpf. K was the lateral view of the in situ hybridization in the spinal cord at 5 dpf. L, M, and N were the three cross-sections of the spinal cord in the rostral to cordial directions at 5 dpf. The DAB color development in B and F was without the nickel enhancement. The arrowhead marked the location of secondary motoneurons. Scale bar was100 μm.

In this study, we show that zebrafish Na$_v$1.6 plays an essential role during the development of embryonic locomotor activities including the in-chorion contraction and tactile contraction. The quantitative PCR revealed that MO3 and MO3mis morphants contains 6% and 25% of the Na$_v$1.6 mRNA relative to that of wild-type embryos. *Med^J* homozygotes with a splice donor mutation in intron 3 of the Na$_v$1.6 gene exhibit the severe muscle weakness, dystonic posture and juvenile lethal, as approximately 6% of the transcripts are correctly spliced [5, 26]. Mutant mice with 12% of the mature Na$_v$1.6 transcripts remained only exhibit the muscle weakness, dystonic posture. *Med^J* heterozygotes with 50% of the normal Na$_v$1.6 transcripts behave like the wild type.

Consistently, MO3-injected embryos exhibit the defective motilities with 6% mature Na$_v$1.6 mRNA. In contrast to MO3 morphants, MO3mis and SMO morphants exhibited the in-chorion contractions like the wild-type embryos. Our data also indicated that 25% of the mature Na$_v$1.6 mRNA in MO3mis morphants was sufficient to elicit these two movements normally.

There are several possibilities that lead to locomotion defects, including the malformation of motor circuits or reduced sodium currents in the neural network. The structure of motor circuits including the axonal projections of CaP primary motoneurons showed no overt differences between control and MO morphants (Figure 4A). The knockdown of Na$_v$1.6 contributed sodium current

was insufficient to affect either the normal morphology or migration of slow muscles as compared with MO3mis and SMO morphants (Figure 4B-a–c). However, the wavy fibers induced by tricaine treatment demonstrated that the electrical activity was necessary for the normal slow-muscle morphology (Figure 4B-d). The majority of AChR clusters were aligned with motoneuron axons in the tricaine-treated embryos, SMO, MO3, and MO3mis morphants. However, Pineda et al. reported that the colocalization of motoneurons and AChR clustering in the distal region of axon was reduced in morphants injected with the splicing-blocking MO in comparison with the control morphants (84 versus 71%). They also showed that the MO delayed in the dorsal projection of $Na_v1.6$ expressing SMN and non-autonomously modulated ventrally projecting SMN, which is absent of $Na_v1.6$. The discrepancy between these two studies may be mainly due to the higher efficiency of their MO than that of MO3 used in this study on the $Na_v1.6$ mRNA splicing blockage. Therefore, more significant phenotypes were observed in their morphants. Secondly, it may be due to the antibody they used for immunohistochemistry. Zn8 visualized the dorsal projecting SMN with little signal detected in the spinal cord. The antigen of antibody znp1 we used expressed highly in the spinal cord, which may hinder our observation of delayed dorsal projecting SMN in the morphants. Thirdly, Tg(gata2:GFP) provided a clear axonal process ventrally projecting SMN than the znp1 immunostaining background we showed here.

Whether the delayed dorsal axonal projection of secondary motoneurons was responsible for the impaired motilities observed in $Na_v1.6$ morphants was examined [12]. We showed that $Na_v1.6$ mRNA levels in secondary motoneuron remained at low abundance until 72 hpf in Figure 5. The spontaneous contraction and tactile sensitivity preceded the expression of $Na_v1.6$ in secondary motoneurons, which excluded the involvement of secondary motoneurons in these two movements. Pineda et al. showed that the axonal projections of secondary motoneurons in the control and morphants just reached the choice point at 48 hpf, therefore, the defective motilities reported here were not resulted from the aberrant axonal projections of secondary motoneurons in $Na_v1.6$ knockdown.

A lack of neuromuscular transmission and paralysis observed in null mice suggests that the sodium currents contributed by $Na_v1.6$ are essential for the normal motor nerve function [5, 26]. The motor nerve conduction velocity is reduced in med^j mice (Kearney et al., 2002). The firing pattern in Purkinje cells of med and Purkinje cell-specific knockout mice of the $Na_v1.6$ gene are defective [6, 7]. It is suggested that both impaired peripheral nerve function and central motor control are involved in the motor dysfunctions exhibited by $Na_v1.6$ mutant mice. Reduced peak sodium currents in RB neurons was also observed by the knockdown of $Na_v1.6$ sodium channels [12]. Our study suggests that the reduced expression of $Na_v1.6$ sodium channels in the motor circuitry was responsible for the embryonic locomotion defects of MO morphants. The knockdown of zebrafish $Na_v1.6$ sodium channels may hinder the production of the periodic depolarization of the network-driven activity of in-chorion coiling and hindbrain/spinal cord mediation of the escape/swimming movements at later stages [27]. Motor nerve conduction velocity and neurotransmitter release should be compared between SMO and MO morphants in the future.

Acknowledgements

References

1. Tzoumaka E., Tischler A.C., Sangameswaran L., Eglen R.M., Hunter J.C. and Novakovic S.D., Differential distribution of the tetrodotoxin-sensitive rPN4/NaCh6/Scn8a sodium channel in the nervous system. J. Neurosci. Res. 60: 37–44, 2000.
2. Caldwell J.H., Schaller K.L., Lasher R.S., Peles E. and Levinson S.R., Sodium channel $Na_v1.6$ is localized at nodes of ranvier, dendrites, and synapses. Proc. Natl. Acad. Sci. U.S.A. 97: 5616–5620, 2000.
3. Krzemien D.M., Schaller K.L., Levinson S.R. and Caldwell J.H., Immunolocalization of sodium channel isoform NaCh6 in the nervous system. J. Comp. Neurol. 420: 70–83, 2000.
4. Burgess D.L., Kohrman D.C., Galt J., Plummer N.W., Jones J.M., Spear B. and Meisler M.H., Mutation of a new

sodium channel gene, Scn8a, in the mouse mutant 'motor endplate disease'. Nat. Genet. 10: 461–465, 1995.

5. Kearney J.A., Buchner D.A., De H.G., Adamska M., Levin S.I., Furay A.R., Albin R.L., Jones J.M., Montal M., Stevens M.J., Sprunger L.K. and Meisler M.H., Molecular and pathological effects of a modifier gene on deficiency of the sodium channel Scn8a ($Na_v1.6$). Hum. Mol. Genet. 11: 2765–2775, 2002.

6. Levin S.I., Khaliq Z.M., Aman T.K., Grieco T.M., Kearney J.A., Raman I.M. and Meisler M.H., Impaired motor function in mice with cell-specific knockout of sodium channel Scn8a ($Na_v1.6$) in cerebellar purkinje neurons and granule cells. J Neurophysiol 96: 785–793, 2006.

7. Raman I.M., Sprunger L.K., Meisler M.H. and Bean B.P., Altered subthreshold sodium currents and disrupted firing patterns in Purkinje neurons of Scn8a mutant mice. Neuron 19: 881–891, 1997.

8. Garcia K.D., Sprunger L.K., Meisler M.H. and Beam K.G., The sodium channel Scn8a is the major contributor to the postnatal developmental increase of sodium current density in spinal motoneurons. J. Neurosci. 18: 5234–5239, 1998.

9. Tsai C.W., Tseng J.J., Lin S.C., Chang C.Y., Wu J.L., Horng J.F. and Tsay H.J., Primary structure and developmental expression of zebrafish sodium channel $Na_v1.6$ during neurogenesis. DNA Cell Biol. 20: 249–255, 2001.

10. Novak A.E., Taylor A.D., Pineda R.H., Lasda E.L., Wright M.A. and Ribera A.B., Embryonic and larval expression of zebrafish voltage-gated sodium channel alpha-subunit genes. Dev. Dyn. 235: 1962–1973, 2006.

11. Pineda R.H., Heiser R.A. and Ribera A.B., Developmental, molecular, and genetic dissection of INa in vivo in embryonic zebrafish sensory neurons. J. Neurophysiol. 93: 3582–3593, 2005.

12. Pineda R.H., Svoboda K.R., Wright M.A., Taylor A.D., Novak A.E., Gamse J.T., Eisen J.S. and Ribera A.B., Knockdown of Nav 1.6a Na^+ channels affects zebrafish motoneuron development. Development 133: 3827–3836, 2006.

13. Saint-Amant L. and Drapeau P., Time course of the development of motor behaviors in the zebrafish embryo. J. Neurobiol. 37: 622–632, 1998.

14. Buss R.R. and Drapeau P., Synaptic drive to motoneurons during fictive swimming in the developing zebrafish. J. Neurophysiol. 86: 197–210, 2001.

15. Svoboda K.R., Linares A.E. and Ribera A.B., Activity regulates programmed cell death of zebrafish Rohon-Beard neurons. Development 128: 3511–3520, 2001.

16. Devoto S.H., Melancon E., Eisen J.S. and Westerfield M., Identification of separate slow and fast muscle precursor cells in vivo, prior to somite formation. Development 122: 3371–3380, 1996.

17. Crow M.T. and Stockdale F.E., Myosin expression and specialization among the earliest muscle fibers of the developing avian limb. Dev. Biol. 113: 238–254, 1986.

18. Downes G.B. and Granato M., Acetylcholinesterase function is dispensable for sensory neurite growth but is critical for neuromuscular synapse stability. Dev. Biol. 270: 232–245, 2004.

19. Saint-Amant L. and Drapeau P., Synchronization of an embryonic network of identified spinal interneurons solely by electrical coupling. Neuron 31: 1035–1046, 2001.

20. Personius K.E. and Balice-Gordon R.J., Activity-dependent editing of neuromuscular synaptic connections. Brain Res. Bull. 53: 513–522, 2000.

21. Bulman D.E., Phenotype variation and newcomers in ion channel disorders. Hum. Mol. Genet. 6: 1679–1685, 1997.

22. Lai J., Gold M.S., Kim C.S., Bian D., Ossipov M.H., Hunter J.C. and Porreca F., Inhibition of neuropathic pain by decreased expression of the tetrodotoxin-resistant sodium channel, $Na_v1.8$. Pain 95: 143–152, 2002.

23. Akopian A.N., Souslova V., England S., Okuse K., Ogata N., Ure J., Smith A., Kerr B.J., McMahon S.B., Boyce S., Hill R., Stanfa L.C., Dickenson A.H. and Wood J.N., The tetrodotoxin-resistant sodium channel SNS has a specialized function in pain pathways. Nat. Neurosci. 2: 541–548, 1999.

24. Escayg A., MacDonald B.T., Meisler M.H., Baulac S., Huberfeld G., An-Gourfinkel I., Brice A., LeGuern E., Moulard B., Chaigne D., Buresi C. and Malafosse A., Mutations of SCN1A, encoding a neuronal sodium channel, in two families with GEFS[+2]. Nat. Genet. 24: 343–345, 2000.

25. Planells-Cases R., Caprini M., Zhang J., Rockenstein E.M., Rivera R.R., Murre C., Masliah E. and Montal M., Neuronal death and perinatal lethality in voltage-gated sodium channel alpha(II)-deficient mice. Biophys. J. 78: 2878–2891, 2000.

26. Meisler M.H., Kearney J., Escayg A., MacDonald B.T. and Sprunger L.K., Sodium channels and neurological disease: insights from Scn8a mutations in the mouse. Neuroscientist 7: 136–145, 2001.

27. Drapeau P., Saint-Amant L., Buss R.R., Chong M., McDearmid J.R. and Brustein E., Development of the locomotor network in zebrafish. Prog. Neurobiol. 68: 85–111, 2002.